

THE KINEMATICS OF PREY CAPTURE IN *XYSTREURYS LIOLEPIS*: DO ALL FLATFISH FEED ASYMMETRICALLY?

ALICE C. GIBB*

Department of Ecology and Evolutionary Biology, University of California, Irvine, CA 92717, USA

Accepted 6 June 1996

Summary

Previous research has shown that one species of flatfish displays several functional asymmetries of the head and jaws during prey capture. However, it is not known whether the functional asymmetries observed for this species are common to all flatfishes. In order to determine whether functional asymmetry is present in other flatfish taxa, prey-capture behavior was examined in a species of flatfish with little cephalic morphological asymmetry, *Xystreurus liolepis* (Pleuronectiformes: Paralichthyidae). In addition, *X. liolepis* is one of a few species of flatfish in which both typical (sinistral) and reversed (dextral) individuals are commonly found. Five individuals (two dextral and three sinistral) of *X. liolepis* were video-taped feeding at 250 fields s⁻¹ in order to quantify prey-capture kinematics. These data were used to test two hypotheses: (1) that typical and reversed-symmetry individuals have identical prey-capture kinematics, and (2) that *X. liolepis* exhibit no functional asymmetry during prey capture because they have little morphological asymmetry. Analysis of prey capture indicates that the kinematic

variables measured for sinistral and dextral individuals are statistically indistinguishable. In addition, *X. liolepis* do not exhibit the same suite of functional asymmetries that has been found in a flatfish species with more extreme cephalic morphological asymmetry (*Pleuronichthys verticalis*). However, asymmetrical anterior movement of the ventral portion of the maxilla does occur in *X. liolepis* during mouth opening. Examination of osteological preparations and cleared and stained individuals indicates that the maxilla is asymmetrical in length in this species. A simple model indicates that the differential length of the maxilla is sufficient to explain the observed functional asymmetry during prey capture. These results suggest that certain morphological asymmetries of the jaws of flatfishes are modifications for specialized prey-capture behaviors.

Key words: prey capture, feeding behavior, kinematics, flatfish, asymmetry, *Xystreurus liolepis*.

Introduction

Pleuronectiform fishes (flatfishes) are a large and successful group of teleost fishes which have deviated from the general vertebrate plan of skeletal and muscular bilateral symmetry. Although flatfishes hatch as bilaterally symmetrical larvae, during metamorphosis one eye migrates to the opposite side of the head (Ahlstrom *et al.* 1984). Flatfish also lose all coloration on the eyeless (blind) side of the body and develop cryptic coloration on the eyed (ocular) side of the body during metamorphosis (Ahlstrom *et al.* 1984). At the end of this developmental period, these fish settle to the bottom and rest on their blind (or eyeless) side. Asymmetrical coloration and eye position allow flatfishes to lie undetected on the bottom while their eyes scan the surrounding environment for potential prey.

Migration of the eye has at least two direct consequences for the symmetry of the cephalic bones and muscles: (1) the neurocranium becomes asymmetrical and contorted because it

‘twists’ towards the ocular (eyed) side during eye migration (Ahlstrom *et al.* 1984), and (2) the musculo-skeletal elements of the jaw apparatus are generally smaller on the ocular side because of the presence of the additional eye (Yazdani, 1969). However, there is much variation in the degree and type of cephalic morphological asymmetry among flatfish taxa. The most plesiomorphic family, the Psettodidae (Chapleau, 1993), apparently exhibits only the morphological asymmetry directly related to eye migration described above (Yazdani, 1969). In contrast, the most derived family, the Cynoglossidae (Chapleau, 1993), displays extreme cephalic morphological asymmetry which appears to represent further modification of the head and jaws beyond that created by eye migration (Yazdani, 1969). Previous researchers have hypothesized that the extreme morphological asymmetry in some flatfish taxa represents modification of the head and jaws for specific feeding behaviors (Hubbs and Hubbs, 1945; Yazdani, 1969).

*e-mail: acgibb@uci.edu.

Can morphological asymmetry predict functional asymmetry?

The flatfish species *Pleuronichthys verticalis* is a member of the tribe Pleuronectini (Pleuronectidae), a group characterized by their small asymmetrical mouths with teeth present only on the blind side of the jaws (Chapleau, 1993). In addition to the neurocranial asymmetry caused by eye migration, *Pleuronichthys verticalis* demonstrate extreme asymmetry of the palatine, maxilla and upper and lower jaws (Gibb, 1995). These particular morphological asymmetries of the head and jaws are apparently associated with two functional asymmetries which occur during prey capture: (1) asymmetrical gape and (2) flexion of the jaws out of the midline of the head (Gibb, 1995). However, so little is known about flatfish prey capture that it is difficult to assess whether these functional asymmetries are specific to *P. verticalis*; it is possible that they are commonly found among many species of flatfish.

Xystreurus liolepis (Paralichthyidae) have less cephalic morphological asymmetry than *P. verticalis*. Thus, a comparison of the feeding behavior between these two taxa will elucidate the relationship between morphological asymmetry and functional asymmetry during prey capture. Since *X. liolepis* appear to have little asymmetry beyond that accounted for by eye migration, they may potentially demonstrate prey-capture behavior that exhibits no functional asymmetries. Therefore, in this study, the prey capture of *X. liolepis* was quantified in order to test the specific hypothesis that this species exhibits a more moderate type of functional asymmetry during prey capture than *P. verticalis* (or possibly none at all). If this hypothesis is not falsified, it will lend support to the overall hypothesis that flatfish cephalic morphological asymmetries are associated with specific functional asymmetries during prey capture.

Do reversed-symmetry flatfish feed like typical-symmetry flatfish?

Flatfish are often characterized by the side of the head on which the eyes are found after metamorphosis. Some species are dextral ('right-handed') and have both eyes on the right side of their head, others are sinistral ('left-handed') and have both eyes on the left side. In most species of flatfish, all the individuals within the species have the same handedness, which implies that this trait is under genetic control (Policansky, 1982a,b). *Xystreurus liolepis* is one of a handful of pleuronectiform species (out of hundreds) in which individuals are often found with reversed asymmetry (Hubbs and Hubbs, 1945; Ginsburg, 1952; Policansky, 1982a). Generally, reversed individuals are found only at a low frequency within a population (Hubbs and Hubbs, 1945).

The significance of the reversal of the typical pattern of symmetry in flatfishes is not known. Since individuals with typical handedness usually dominate the population (by definition), it is possible that individuals which are reversed are at some potential disadvantage. Two potential disadvantages for reversed individuals have been proposed: (1) reversed

individuals may have difficulty reproducing with typical individuals (because male flatfish lie on top of female flatfish in order to align cloacas during mating) or (2) the optic chiasma of reversed individuals crosses twice (it only crosses once in typical individuals) (Policansky, 1982a). There is no empirical evidence from either field or laboratory studies to support either of these two ideas.

Reversed individuals of any flatfish species appear to be completely morphologically reversed with two exceptions: (1) the optic chiasma in reversed individuals crosses twice (as described above) and (2) flatfish always follow one pattern for positions of the internal organs. In flatfishes, as in most other fishes, the intestinal coils always reside against the right body wall, and the liver always lies against the left (Hubbs and Hubbs, 1945). In contrast, all the skeletal and muscular features of the body are mirror images in reversed individuals.

Reversed individuals of *X. liolepis* are present at a low frequency within the population resident off the Pacific coast of North America. In this study, two reversed individuals were compared with three typical individuals to test the hypothesis that there are no functional differences between reversed individuals and typical individuals during prey capture. Similarities in feeding performance, as measured by the kinematics of prey capture, will be taken as evidence that reversed flatfish are able to feed as successfully as typical individuals in their natural habitat.

Materials and methods

Species used in the study

Xystreurus liolepis (Jordan and Gilbert) were chosen for this study for several reasons. First, this species has little cephalic asymmetry (A. C. Gibb, personal observation) when compared with other flatfishes. Second, reversed-symmetry individuals of *X. liolepis* could be obtained. Third, individuals of *X. liolepis* could be closely size-matched with individuals used in a previous feeding study of another flatfish, *Pleuronichthys verticalis* (Gibb, 1995). Fourth, *X. liolepis* were usually captured in the same bottom trawls as *P. verticalis* and thus represent a potentially interesting ecological comparison of prey-capture strategies. In addition, this species feeds readily in a laboratory environment and could be obtained locally.

Xystreurus liolepis are considered to be generalist predators, although much of their diet consists of small crustaceans (Allen, 1982; Kramer, 1991). In the laboratory, these animals fed readily on prey items of all types (both elusive and non-elusive). Earthworms, *Lumbricus terrestris*, were used as prey in this study for three reasons: (1) the fish feed readily on them in the laboratory, (2) they are good models of the soft-bodied invertebrates that are included in the diet of this species, and (3) they had been used as the prey in a previous study of flatfish feeding (Gibb, 1995) and this eliminated any potential effects of prey type on comparisons made across taxa.

Collection and maintenance of specimens

Xystreurus liolepis were collected during otter trawls

conducted at 30 m depths off the coast of Orange County, California. Individuals which died as a result of the trawl were used for anatomical description. The head and jaws of fresh dead specimens were manipulated and dissected in order to observe passive movements of bones and muscles. Specimens used for other types of anatomical description were either frozen until needed for dissection or chemically preserved by immersion in buffered formalin for several days and then transferred to a 70% ethanol solution. Frozen specimens were thawed, and individual bones were cleaned, removed from the head and used as osteological preparations. Chemically preserved specimens were cleared and stained in order to describe the cephalic bones and cartilage of intact individuals.

Specimens captured alive and in good condition were transferred to the laboratory, where they were maintained in 80 l saltwater aquaria at a temperature of 18–20 °C and with a 12 h:12 h light:dark cycle. The video-taping chamber used in this study was a 120 l saltwater aquarium (dimensions 90 cm×30 cm×30 cm) with a transparent bottom and was maintained at a temperature of 20±1 °C. Fish were transferred to this chamber at least 48 h prior to video-taping and allowed to acclimate to it.

Video-taping and digitizing

Five individual *Xystreureys liolepis* were video-taped using a NAC high-speed video system at 250 fields s⁻¹. Three sinistral individuals were used for the video-taping (size range: standard length 16.2–18.2 cm, head length 4.4–4.7 cm) and two dextral individuals (size range: standard length 14.9 and 15.6 cm, head length 3.9 and 4.1 cm). Individual *X. liolepis* were fed earthworm pieces approximately 2 cm in length placed on the bottom of the chamber. Feeding events were video-taped using similar methods to those used in the analysis of *P. verticalis* prey capture (Gibb, 1995). Three views of prey capture were recorded: (1) a view of the ocular side reflected from a front-surface mirror placed at 45° above the tank, (2) a view of the blind side reflected from a front-surface mirror placed at 45° below the tank, and (3) a view of the gular region recorded using a camera placed perpendicular to the front of the chamber. For the gular view, only sequences in which the long axis of the fish was parallel to the front of the filming tank were accepted. The three views were recorded using the two-camera video system in the following combinations: ocular and blind views were recorded together, as were gular and blind views. Eight prey-capture events were recorded and analyzed for each individual (four feeding events using each combination of views).

Video images were analyzed using a custom-designed digitizing program. Points on the neurocranium, jaws, hyoid and opercles were digitized, as well as several reference points on the body. At least 29 frames (which comprised 720 ms total elapsed time) were analyzed for each feeding sequence. *X. liolepis* displayed variation in their behavior while approaching the prey. Some individuals (in some sequences) approached the prey from a great distance with their mouths slightly agape. Other individuals (or the same individuals in other sequences)

did not open their mouths until immediately before prey capture. All individuals, in all sequences, demonstrated rapid mouth opening immediately before prey capture, and it was during this period that other important kinematic events occurred (e.g. cranial rotation). Therefore, for all prey-capture sequences, time 0 was defined as the time at which the mouth began to open rapidly. The 29 frames analyzed for each prey-capture event included the following times during the feeding cycle: -416 ms to time 0 (in 32 ms intervals), time 0 to 88 ms (in 8 ms intervals), 88 ms to 152 ms (in 32 ms intervals), 200 ms and 304 ms.

Kinematic variables

After the video sequences had been digitized, the coordinates of digitized points were used to calculate a total of 18 kinematic variables. All movements of the head and jaws during feeding were determined relative to the anatomical orientation of the fish. All of the variables (with the exception of maximum maxilla angle) were calculated using methods identical to those in the previous study of flatfish feeding (Gibb, 1995).

Seven variables associated with the displacement and timing of movements of the jaws during prey capture were calculated: (1) maximum gape (cm), the maximum distance between the upper and lower jaws; (2) the time to maximum gape (ms), the interval between the beginning of rapid mouth opening and maximum gape; (3) gape cycle time (ms), the total time the mouth was open; (4) maximum depression of the lower jaw (degrees), the maximum angle calculated between three points: a point on the anterior tip of the lower jaw, a point near the articulation of the lower jaw with the quadrate and a point at the base of the pectoral fin; (5) time to maximum lower jaw depression (ms), the interval between the beginning of rapid mouth opening and maximum lower jaw depression; (6) maximum upper jaw protrusion (cm), the maximum anterior displacement of the premaxilla; and (7) time to maximum protrusion of the upper jaw (ms), the interval between the beginning of rapid mouth opening and maximum upper jaw protrusion.

Two variables describing movements of the neurocranium were measured. Cranial rotation (degrees) during prey capture (termed 'head elevation' or 'cranial elevation' in previous studies) was measured as the angular rotation of the neurocranium dorsally relative to the body. The angle of the neurocranium was determined using three points: a point on the neurocranium near the articulation of the premaxilla, a point on the neurocranium near the attachment of the dorsal fin and a point at the base of the pectoral fin. Time to maximum cranial rotation (ms) was calculated as the interval between the beginning of rapid mouth opening and the time of maximum cranial rotation.

Four variables describing movements of the hyoid were also calculated. Maximum hyoid depression (cm) was determined using the most ventral position of the hyoid during prey capture, and maximum hyoid retraction (cm) was determined by its most posterior position. The intervals between the

beginning of rapid mouth opening and the most depressed and retracted positions of the hyoid were calculated as the time to maximum hyoid depression (ms) and time to maximum hyoid retraction (ms), respectively.

Two variables quantified timing and displacement of the opercular series during prey capture. Maximum opercular expansion (cm) occurred when the ocular and blind side opercles were maximally laterally displaced. The time to maximum opercular expansion (ms) was calculated as the interval between the beginning of rapid mouth opening and the maximum lateral expansion of the opercular series.

Of the 15 variables described above, six involved unpaired structures. Since unpaired structures cannot move in a bilaterally asymmetrical manner, the following variables were quantified from the blind-side view only: maximum hyoid depression, time to maximum hyoid depression, maximum hyoid retraction, time to maximum hyoid retraction, maximum cranial rotation and time to maximum cranial rotation. However, nine of the timing and displacement variables involved movements of paired structures with the potential for functional asymmetry. These variables were calculated for both the blind and the ocular sides of the head: maximum gape, time to maximum gape, gape cycle time, maximum upper jaw protrusion, time to maximum upper jaw protrusion, maximum lower jaw depression, time to maximum lower jaw depression, maximum opercular expansion and time to maximum opercular expansion.

An additional variable was measured from the ocular- and blind-side views during the feeding of *X. liolepis* because preliminary analysis of the video tapes suggested that asymmetry might be present: maximum maxilla angle (degrees). This angle was defined by three points: the anterior tip of the premaxilla, the most anterior point on the ventral process of the maxilla and the anterior tip of the mandible.

Two other angular variables were measured for *X. liolepis* prey capture. These variables were calculated from the gular view and examined the head and jaws for potentially asymmetrical movements: maximum lateral flexion of the head (degrees) (the angle formed by a point at the base of the pectoral fin, a posterior point on the eye and a line parallel with the bottom) and maximum lateral flexion of the lower jaw (degrees) (the angle formed by a point on the anterior apex of the lower jaw, a point at the base of the lower jaw and a line parallel with the midline of the head). Lateral flexion towards the blind side of the head was considered to be a negative angle; lateral flexion towards the ocular side was considered to be a positive angle.

Statistical analyses

Two sets of statistical analyses were performed in this study. One analysis examined the data for potential differences between sinistral and dextral individuals of *X. liolepis*. The other analysis examined the data for potential functional asymmetries or side-of-the-head effects (i.e. differences between the ocular and blind sides of the head). Handedness (sinistral *versus* dextral individuals) and side-of-the-head

(ocular- *versus* blind-side variables) were considered to be fixed effects and individual was treated as a random effect in all analyses of variance.

It was not possible to perform a generalized multivariate analysis of variance (MANOVA) on the complete data set because the number of kinematic variables in the study exceeds the number of observations. Therefore, a principal components analysis (PCA) was used to examine 24 kinematic variables (see Table 1) for the sinistral and dextral individuals. This analysis provided a multivariate summation of the patterns of variation in the data set to be used in the MANOVA. The MANOVA was performed on the first two principal component factors (PC1 and PC2) to test the null hypothesis that there was no difference between the sinistral and dextral individuals in overall prey-capture kinematics. The PCA was performed using Systat for the Macintosh and the MANOVA was performed using SuperANOVA for the Macintosh.

Although the MANOVA was non-significant (see Results), there was a trend for PC1 of the PCA to separate the sinistral and dextral individuals into two groups. In order to determine which variables were contributing to this result, the unpaired and paired kinematic variables measured for both sides of the head were examined individually for potential effects of 'handedness' (sinistral *versus* dextral) in a nested ANOVA. In this analysis, individual was considered to be nested within handedness; the individual mean square was used to calculate the *F*-statistic for handedness and the residual was used to calculate the *F*-statistic for the individual.

When no statistically significant differences were found in the first analyses (see Results), the data for sinistral and dextral individuals were combined, and a second set of ANOVAs was performed on the combined data set to examine the variables specifically for individual variation and functional asymmetry. Multiple one-way ANOVAs were performed on the unpaired variables to examine them for potential individual variation. Multiple mixed-model two-way ANOVAs examined the combined data set for side-of-the-head and individual effects. In addition to the other kinematic variables analyzed for potential functional asymmetry, one additional variable (the maximum maxilla angle) was also analyzed using a two-way ANOVA model. The *F*-statistics for the two-way ANOVAs were calculated as follows: individual was tested over the residual, side-of-the-head was calculated over the interaction term of individual and side-of-the-head, and the interaction term was calculated over the residual. All ANOVAs were calculated using the program SuperANOVA for the Macintosh.

Unpaired *t*-tests were performed on head and jaw lateral flexion. The null hypothesis for these tests was that there was no lateral bending of the head or body (angle=0°). Qualitative analysis of the data indicated that the head of *X. liolepis* could potentially bend towards the ocular or the blind side, so two-tailed *t*-tests were used to analyze the data. All *t*-tests were performed using the Macintosh program Statview.

To account for multiple simultaneous ANOVAs, levels of statistical significance were adjusted for all ANOVAs and *t*-tests using the sequential Bonferroni technique (Rice, 1989).

However, since two separate analyses were performed, two sets of sequential Bonferroni corrections were performed. A correction was performed for the multiple nested ANOVAs examining the data for potential effects of handedness (total 24 tests). When the data were combined for the analysis of potential effects of individual variation and side-of-the-head effects (i.e. functional asymmetry), a second sequential Bonferroni correction was performed on these multiple two-way ANOVAs and *t*-tests (total 18 tests total; 16 ANOVAs and two *t*-tests).

Results

Morphological asymmetry

A brief description of the cephalic morphology of *X. liolepis* is given here as a basis for understanding prey-capture kinematics and functional asymmetry. *Xystreurys liolepis* have a more moderate degree of morphological asymmetry than that

found in many other flatfishes (Yazdani, 1969; Gibb, 1995). Much of the asymmetry found in the skull appears to be associated with the twisting of the neurocranium that occurs during eye migration (Fig. 1). The maxilla, premaxilla and lower jaw, structures previously found to be extremely asymmetrical in shape and size in *P. verticalis* (Gibb, 1995), exhibit little or no asymmetry in *X. liolepis* (Fig. 1).

Two exceptions to this trend of little or no asymmetry are present in *X. liolepis*. The maxilla is consistently longer (although it is a similar shape) on the ocular side of the head than on the blind side of the head in *X. liolepis* (Fig. 2B). This asymmetry is opposite to the typical flatfish pattern of having larger bones and muscles on the blind side of the head (Yazdani, 1969). Another bone which displays notable asymmetry in its size and shape is the palatine. It is smaller and has a different shape on the ocular side of the head (Fig. 2A). However, the anterior process of the ocular-side

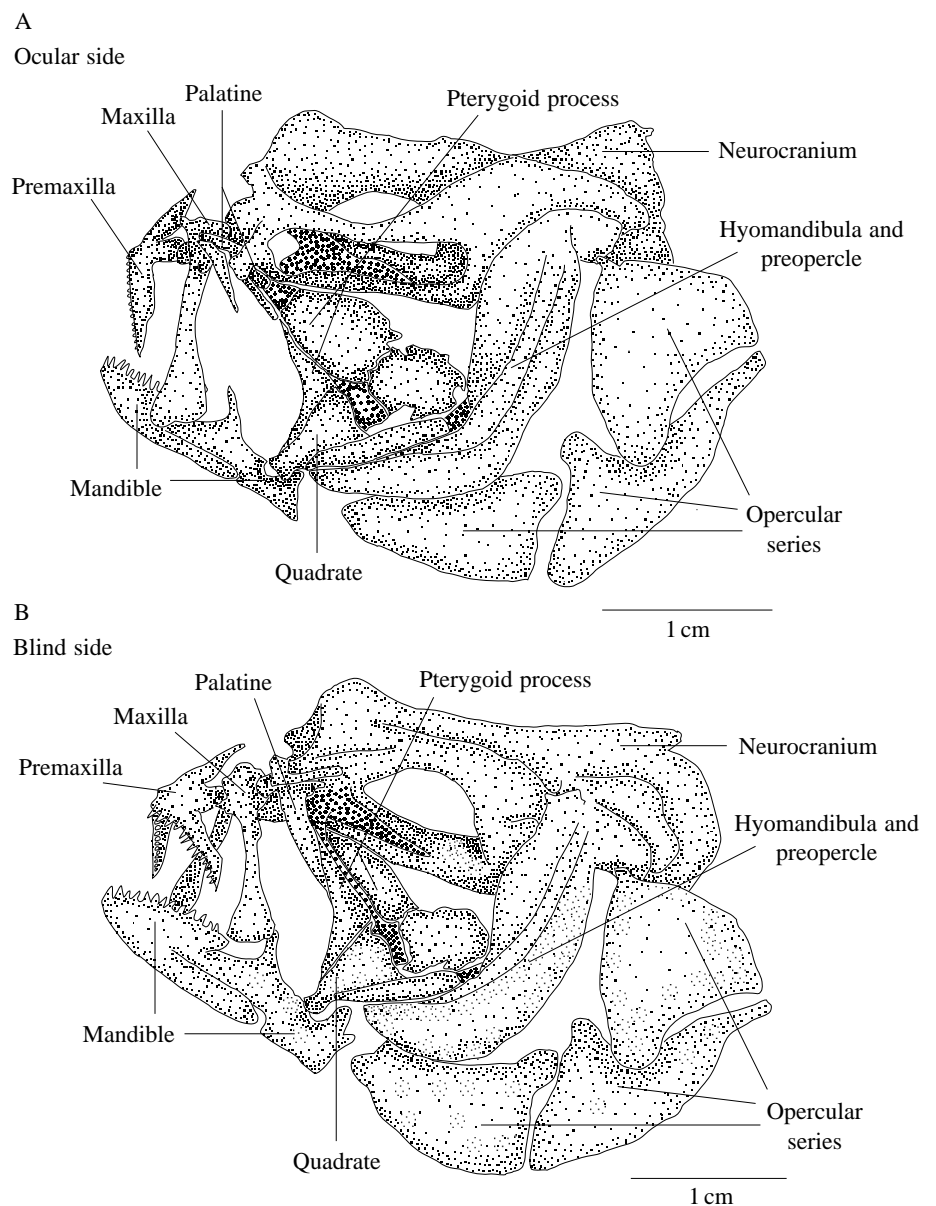


Fig. 1. *Camera lucida* drawings of a cleared and stained skull of a sinistral *Xystreurys liolepis*. (A) The ocular side of the head; (B) the blind side. Note that the blind side has been reversed horizontally in order to facilitate comparisons with the ocular side. Little or no asymmetry is present in the following bones: premaxilla, mandible, suspensorium and opercular series. The maxilla and palatine bone, however, are asymmetrical in nature.

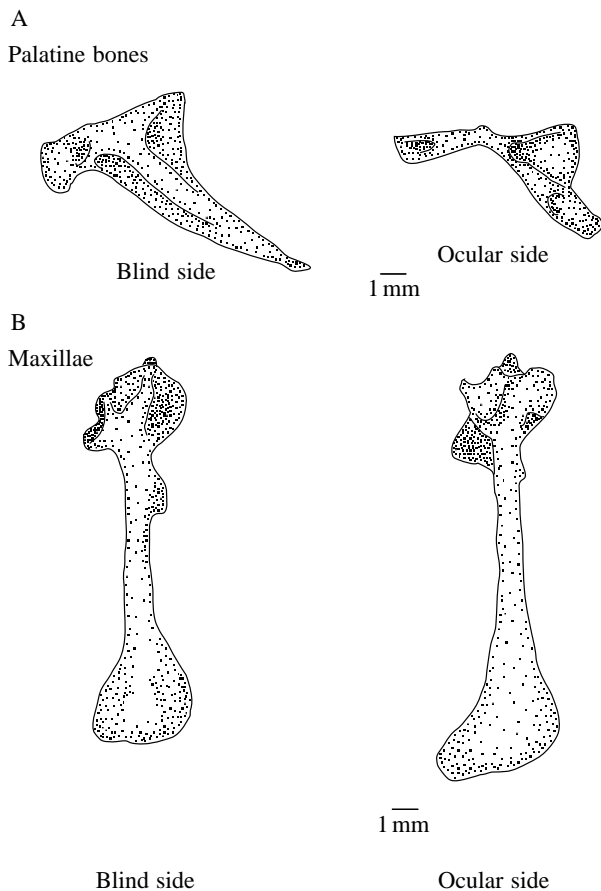


Fig. 2. *Camera lucida* drawings of isolated bones from a dissected sinistral specimen of *Xystreureys liolepis*. (A) The palatine bones; (B) the maxillae. Bones from the blind side of the head are pictured on the left, bones from the ocular side of the head are on the right. Palatine bones and maxillae are drawn from a lateral view. Note that the bones from the blind side have been reversed horizontally in order to facilitate comparisons with the ocular side. The maxilla is significantly longer on the ocular side of the head, and the palatine bone has a longer anterior process on the ocular side.

palatine bone is longer than the anterior process of the blind-side palatine bone, and its head is a different shape.

One other asymmetry of the jaws of *X. liolepis* is apparent in the cleared and stained individuals and fresh dead individuals. When the mouth is slightly agape in these specimens, the bones of the upper jaw (the maxilla and the premaxilla) are in a more anterior position on the ocular side of the head than on the blind side of the head (Fig. 1).

General kinematics of prey capture

Xystreureys liolepis approached their prey from a distance with their jaws slightly agape (Figs 3, 4), although this was not always the case. Individuals generally approached the prey rapidly by swimming just off the bottom of the tank (Fig. 4). When the fish were within approximately 2 cm of the prey, they began rapid mouth opening and lower jaw depression (Fig. 4, 0–16 ms) and bent their heads slightly towards the prey item, apparently to facilitate engulfing it (Fig. 4, 16–32 ms).

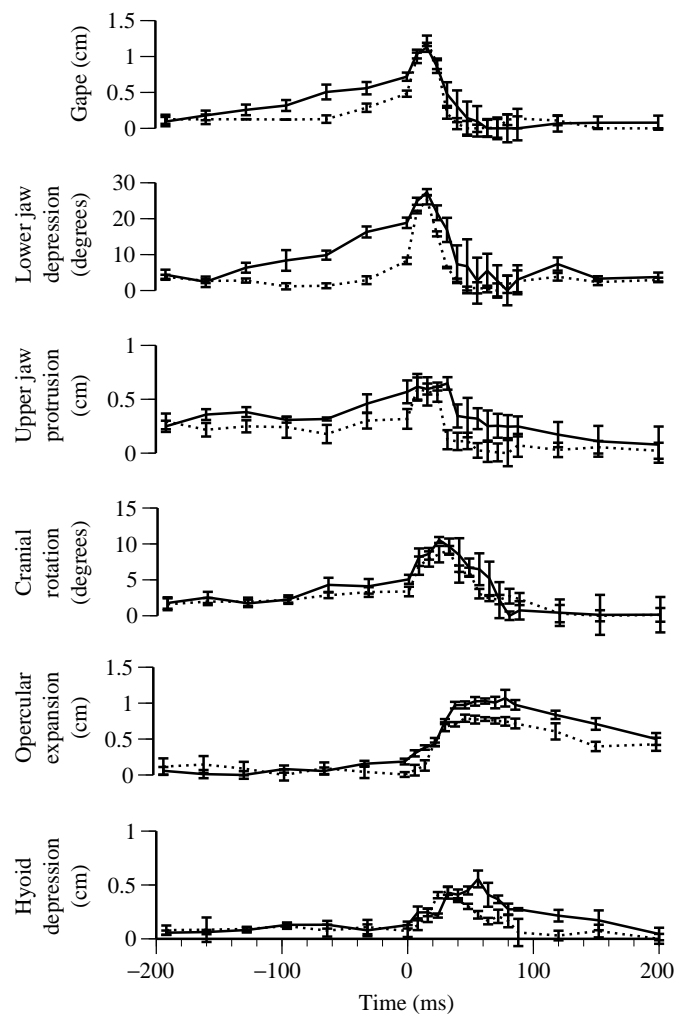


Fig. 3. Kinematic profiles for one sinistral (XLS2; solid line) and one dextral (XLD4; dotted line) *Xystreureys liolepis*. Points on the line represent the mean values for four combined feeding sequences for one individual; error bars represent one standard error of the mean. Time 0 is defined as the beginning of rapid mouth opening.

Xystreureys liolepis achieved maximum gape between 30 and 35 ms after the beginning of rapid mouth opening; the total gape cycle time was approximately 80 ms (Fig. 3). Maximum cranial rotation occurred at the same time as peak gape or shortly thereafter (Fig. 3). Maximum hyoid depression occurred at the very end of mouth closing or after the mouth had already closed (Fig. 3). Gape, lower jaw depression and upper jaw protrusion all reached their maxima at approximately the same time during the gape cycle. One other notable feature of prey capture in *X. liolepis* was the large amount of expansion that occurred in the opercular series, suspensorium and jaws during prey capture (compare the gular views at 0 and 48 ms in Fig. 4).

Reversed- and typical-symmetry individuals

The general pattern of cephalic movements during prey capture is very similar in sinistral and dextral individuals.

Fig. 4. Selected video frames from a representative prey-capture sequence for one sinistral *Xystreurus liolepis* (XLS2). Video images have been cropped and the contrast has been manipulated to increase the clarity of the image. The gular view is presented in the top half of each panel and the blind-side view in the bottom half. Time is given in milliseconds, with time 0 considered to be the beginning of rapid mouth opening.

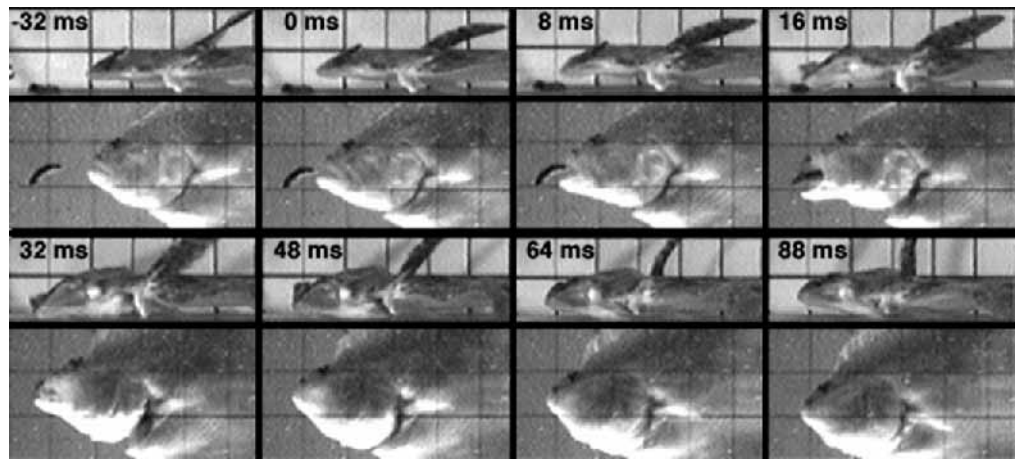


Fig. 3 illustrates the mean displacement of six representative kinematic variables during four feeding events for one sinistral individual and one dextral individual. Even though these individuals are slightly different sizes (the sinistral individual was 1.3 cm longer in standard length), they show remarkably similar amplitude and timing of all kinematic variables. The only qualitative difference in the feeding behavior of these two individuals was that this sinistral individual had a tendency to approach the prey with its mouth open (greater gape early in the cycle, Fig. 3), whereas the dextral individual was more likely to approach the prey with its mouth closed (smaller gape early in the cycle, Fig. 3). This difference in behavior probably also contributed to the slight differences in the amount of lower jaw depression and upper jaw protrusion between sinistral and dextral individuals. However, this result is simply a behavioral difference between these individuals and did not appear as a consistent trend; during some feeding events sinistral individuals approached their prey with their mouths closed, and during some events dextral individuals approached the prey with their mouths open.

The MANOVAs performed on the first two principal components factors (PC1 and PC2) for the 24 kinematic variables (Table 1) indicated no significant overall difference in prey-capture kinematics between the sinistral and dextral individuals (d.f.=2, 2; F -value=2.60; Wilks' lambda $P=0.28$). However, when PC1 was plotted *versus* PC2, the prey-capture events were separated into two groups by PC1 with only a small degree of overlap. All of the paired variables associated with timing of movements of the upper and lower jaw loaded highly in PC1 (gape cycle time, time to maximum gape, time to maximum upper jaw protrusion and time to maximum lower jaw depression). Sinistral individuals tended to have positive scores and dextral individuals tended to have negative scores in PC1. In contrast, PC2 did not separate the sinistral and dextral individuals, and the only variables which loaded highly were variables describing maximum gape.

The multiple nested ANOVAs performed on the data showed a similar result: there was a non-significant trend suggesting that the kinematics of sinistral and dextral individuals were different, but these non-significant trends

were present only in timing variables. Unpaired kinematic variables for the sinistral and dextral individuals of *X. liolepis* showed some minor variations in their mean values (Table 1), but none showed a significant effect due to handedness in the nested ANOVA (Table 2). Individual was also not a significant effect (Table 2) for the unpaired kinematic variables. Similarly, the mean values for the paired kinematic variables measured from the ocular and blind sides (Table 1) were not significantly different between the sinistral and dextral individuals (Table 2). There was significant individual variation in the values measured for maximum gape, but not in any of the other variables (Table 2). It is worth noting that even if the Bonferroni corrections were not made, and $P<0.05$ was used as the criterion for significant differences in all tests, the sinistral and dextral individuals would still not show any significant differences in the kinematic variables. It appears that sinistral and dextral individuals are not significantly different in the kinematic parameters of their prey capture. In addition, the non-significant trends in the data suggest that dextral individuals (the reversed individuals) are actually faster than sinistral individuals (Table 1). This is the opposite of what would be predicted if reversed animals were at some functional disadvantage.

Because there were no statistically significant differences between kinematic variables from sinistral and dextral individuals of *X. liolepis*, the data were combined and a detailed analysis was performed on the combined data set to determine whether functional asymmetry was present. This combined data set allowed more degrees of freedom for the analysis of potential side-of-the-head and individual effects.

Functional asymmetry

The combined mean values for the unpaired variables of the sinistral and dextral *X. liolepis* are given in Table 3. One-way ANOVAs on the combined data set confirms that there is no significant individual variation in these data (Table 4). Mean values for the paired variables from the combined data set are given in Table 5. Multiple two-way ANOVAs performed on the paired variables also confirmed the finding that there are no significant asymmetries in these variables (Table 6) with

Table 1. Mean and standard error of the mean for kinematic variables measured for *Xystreureys liolepis* for sinistral and dextral individuals

Variable	Sinistral (N=12)		Dextral (N=8)	
	Mean	S.E.M.	Mean	S.E.M.
Unpaired variables				
Maximum hyoid depression (cm)	0.59	0.03	0.60	0.05
Time to maximum hyoid depression (ms)	87.7	10.3	43.0	4.5
Maximum hyoid retraction (cm)	0.71	0.07	0.59	0.05
Time to maximum hyoid retraction (ms)	37.5	4.3	54.0	7.1
Maximum cranial rotation (degrees)	13.7	0.8	10.8	0.7
Time to maximum cranial rotation (ms)	65.0	9.3	40.0	5.7
Variables measured from the blind side				
Maximum gape (cm)	1.13	0.08	0.84	0.04
Time to maximum gape (ms)	37.2	6.4	25.5	5.0
Gape cycle time (ms)	95.0	10.0	44.0	5.4
Maximum upper jaw protrusion (cm)	0.64	0.05	0.62	0.10
Time to maximum upper jaw protrusion (ms)	41.5	6.5	28.5	6.5
Maximum lower jaw depression (degrees)	31.9	3.0	35.0	1.6
Time to maximum lower jaw depression (ms)	35.0	6.8	7.0	4.8
Maximum opercular expansion (cm)	0.72	0.04	0.48	0.07
Time to maximum opercular expansion (ms)	114.8	10.2	103.0	10.1
Variables measured from the ocular side				
Maximum gape (cm)	1.13	0.07	0.79	0.05
Time to maximum gape (ms)	38.0	4.6	24.5	5.2
Gape cycle time (ms)	89.6	10.3	44.0	5.4
Maximum upper jaw protrusion (cm)	0.78	0.06	0.62	0.05
Time to maximum upper jaw protrusion (ms)	28.5	6.5	32.0	5.5
Maximum lower jaw depression (degrees)	32.6	3.6	37.9	1.4
Time to maximum lower jaw depression (ms)	34.3	6.2	31.0	4.9
Maximum opercular expansion (cm)	0.68	0.05	0.55	0.04
Time to maximum opercular expansion (ms)	114.7	8.1	104.0	11.3

Table 2. F-statistics obtained from multiple nested analyses of variance comparing variables obtained for sinistral and dextral *Xystreureys liolepis*

Variable	Individual (nested within handedness)	
	Handedness d.f.=1, 3	d.f.=3, 15
Unpaired variables		
Maximum hyoid depression (cm)	0.02	1.87
Time to maximum hyoid depression (ms)	8.25	1.48
Maximum hyoid retraction (cm)	0.70	3.68
Time to maximum hyoid retraction (ms)	2.27	2.44
Maximum cranial rotation (degrees)	8.67	0.68
Time to maximum cranial rotation (ms)	3.08	1.43
Variables measured from the blind side		
Maximum gape (cm)	1.76	11.72*
Time to maximum gape (ms)	1.29	1.44
Gape cycle time (ms)	8.30	3.34
Maximum upper jaw protrusion (cm)	0.02	0.79
Time to maximum upper jaw protrusion (ms)	1.47	1.33
Maximum lower jaw depression (degrees)	0.18	7.52
Time to maximum lower jaw depression (ms)	0.72	1.06
Maximum opercular expansion (cm)	9.26	0.93
Time to maximum opercular expansion (ms)	0.64	0.96
Variables measured from the ocular side		
Maximum gape (cm)	3.37	6.92
Time to maximum gape (ms)	2.41	1.68
Gape cycle time (ms)	6.19	3.12
Maximum upper jaw protrusion (cm)	4.98	0.74
Time to maximum upper jaw protrusion (ms)	0.43	3.71
Maximum lower jaw depression (degrees)	0.73	2.24
Time to maximum lower jaw depression (ms)	0.10	1.63
Maximum opercular expansion (cm)	2.78	2.16
Time to maximum opercular expansion (ms)	3.84	0.14

*Significant at $P < 0.05$, using the sequential Bonferroni method described in Rice (1989).

one exception (maximum maxilla angle). In addition, there was no significant interaction of individual and side-of-the-head. There was individual variation in four of the paired kinematic variables: maximum gape (the same variable found to contain significant individual variation in the preliminary analysis), gape cycle time, maximum lower jaw depression and maximum opercular expansion.

Xystreureys liolepis also showed little functional asymmetry

Table 3. Mean and standard error of the mean for kinematic variables measured for unpaired structures for all individuals of *Xystreureys liolepis*

Variable	Mean	S.E.M.
Maximum hyoid depression (cm)	0.59	0.03
Time to maximum hyoid depression (ms)	69.8	8.1
Maximum hyoid retraction (cm)	0.66	0.05
Time to maximum hyoid retraction (ms)	44.1	4.2
Maximum cranial rotation (degrees)	12.5	0.64
Time to maximum cranial rotation (ms)	55.0	6.5

N=20.

Table 4. F-statistics obtained from multiple one-way analyses of variance examining potential individual effects on unpaired kinematic variables for all individuals of *Xystreureys liolepis*

Variable	Individual d.f. 4, 15
Maximum hyoid depression (cm)	1.41
Time to maximum hyoid depression (ms)	4.15
Maximum hyoid retraction (cm)	3.40
Time to maximum hyoid retraction (ms)	3.21
Maximum cranial rotation (degrees)	2.00
Time to maximum cranial rotation (ms)	2.18

*There were no significant individual effects at $P < 0.05$, using the sequential Bonferroni method described in Rice (1989).

Table 5. Mean and standard error of the mean for variables for all individuals of *Xystreureys liolepis* for the ocular and blind sides of the head

Variable	Ocular		Blind	
	Mean	S.E.M.	Mean	S.E.M.
Maximum gape (cm)	0.99	0.06	1.02	0.06
Time to maximum gape (ms)	32.6	3.7	32.5	4.4
Gape cycle time (ms)	75.9	8.7	79.7	9.0
Maximum upper jaw protrusion (cm)	0.72	0.04	0.63	0.05
Time to maximum upper jaw protrusion (ms)	38.0	4.7	36.3	4.8
Maximum lower jaw depression (degrees)	34.7	2.26	33.1	1.91
Time to maximum lower jaw depression (ms)	33.0	4.1	31.8	4.5
Maximum opercular expansion (cm)	0.63	0.03	0.63	0.04
Time to maximum opercular expansion (ms)	99.6	7.9	96.1	8.8
Maximum maxilla angle (degrees)	174.6	2.0	67.7	4.0

N=20.

Table 6. F-statistics obtained from multiple two-way analyses of variance for all individuals of *Xystreureys liolepis* examining variables obtained for the ocular and blind sides of the head and body for potential functional asymmetry

Variable	Side × individual		
	Side d.f.=1, 4	Individual d.f.=4, 30	individual d.f.=3, 30
Maximum gape (cm)	0.16	23.21*	1.51
Time to maximum gape (ms)	0.01	3.56	0.07
Gape cycle time (ms)	5.47	16.49*	0.04
Maximum upper jaw protrusion (cm)	2.54	1.22	0.67
Time to maximum upper jaw protrusion (ms)	0.11	3.64	0.76
Maximum lower jaw depression (degrees)	1.83	6.30*	0.23
Time to maximum lower depression (ms)	0.22	2.02	0.18
Maximum opercular expansion (cm)	0.58	5.14*	0.83
Time to maximum opercular expansion (ms)	0.01	0.97	0.16
Maximum maxilla angle (degrees)	435.33*	2.73	1.74

*Significant at $P < 0.05$, using the sequential Bonferroni method described in Rice (1989).

in lateral flexion of the head and jaws. There was some lateral flexion of the head during prey capture, but there was no consistent direction of the flexion. In some sequences, fish flexed their heads towards the bottom (blind side) to capture the prey item (as shown in Figs 4, 5). In other sequences, fish captured the prey before it settled to the bottom and flexed their heads up off the bottom (towards the ocular side) to engulf it. This resulted in mean lateral head flexion of $4.1 \pm 3.3^\circ$. This amount of mean lateral head flexion was not significantly different from zero (t -value 0.936, critical value 2.093).

Little, if any, flexion of the jaws occurred (mean value $0.9 \pm 1.0^\circ$) and there was no consistent pattern of directionality in the flexion. Therefore lateral jaw flexion was also not significantly asymmetrical (t -value 1.236, critical value 2.093). What little flexion was measured may have been a measurement artifact created by the lateral flexion of the head (Figs 4, 5).

One variable was an exception to the pattern of no functional asymmetry in the kinematic variables: maximum maxilla angle. Fig. 6 shows the asymmetry in the appearance of the mouth during prey capture. The view of the blind side of the head shows a 'V' created by lower jaw depression throughout much of prey capture (Fig. 6, -32 to 64 ms). This 'V' is an angle defined by three points: the anterior tip of the premaxilla, the tip of the ventral process of the maxilla (the vertex) and the anterior tip of the mandible. In contrast to the blind side, in the view of the ocular side this 'V' becomes obscured between 16 and 32 ms after the beginning of rapid mouth opening. This

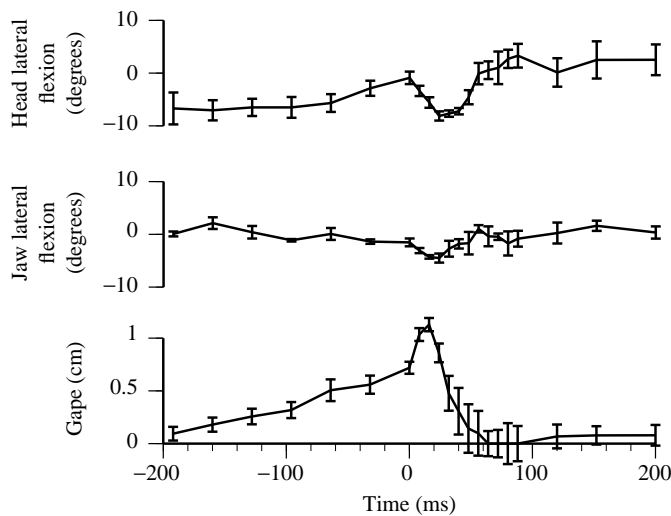


Fig. 5. Summary plot of the angular movements of the jaws and head of one sinistral *Xystreuryx liolepis* (XLS3). Points on the line represent the mean values for four combined feeding sequences for one individual; error bars represent one standard error of the mean. Time 0 is defined as the beginning of rapid mouth opening. Positive values indicate flexion towards the ocular side of the body and negative values indicate flexion towards the blind side.

asymmetry, as described by the maxilla angle, occurred at approximately the same time as maximum cranial rotation and after maximum lower jaw depression (Fig. 7). Table 5 shows that the mean maximum maxilla angle for the blind side was less than 90° (and never exceeded 115°) and the mean maxilla angle for the ocular side approached 180° (a value of 180° would indicate that the anterior tips of the premaxilla, maxilla

and mandible are all in line with one another). This result was highly significant (Table 6).

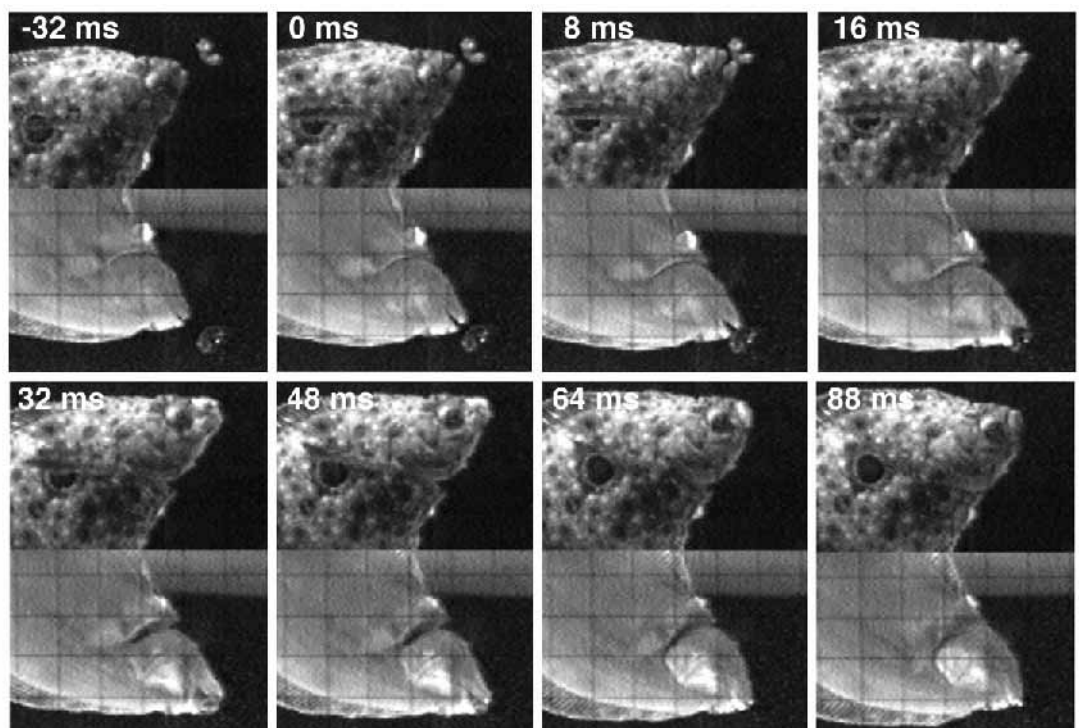
Discussion

Prey capture in reversed- and typical-symmetry individuals

Results from this study support the hypothesis that reversed flatfish individuals are not functionally different from individuals with the typical handedness present in the population. No significant differences were found in prey-capture kinematics between sinistral and dextral individuals. Sinistral and dextral individuals have the same maximum values for kinematic variables, and where mean values differed the trend was that dextral (the reversed individuals) were slightly faster than the sinistral individuals (Table 1; for example, gape cycle time). However, differences in the speed of kinematic events were not significant. These differences could simply be due to the fact that the dextral individuals were slightly smaller than the sinistral individuals, and smaller fish are often faster than larger ones (for example, Richard and Wainwright, 1995). Alternatively, the small sample sizes may be confounding the results; two fast dextral individuals and three slow sinistral individuals may have been chosen for the study by chance alone. In any case, since speed is one way to estimate the performance of an animal during prey capture, these data indicate that dextral individuals (the reversed individuals) are clearly not at a disadvantage when compared with sinistral individuals.

These results do not begin to address the question of why some species of flatfish contain reversed individuals and others do not; that is a question which only further studies of the genetic, developmental and environmental control of the

Fig. 6. Selected video frames from a representative prey-capture sequence for one sinistral *Xystreuryx liolepis* (XLS1). Video images have been cropped and the contrast has been manipulated to increase the clarity of the image. The ocular-side view is presented in the top half of each panel and the blind-side view in the bottom half. Time is given in milliseconds, with time 0 considered to be the beginning of rapid mouth opening. Note that the 'V' created by lower jaw depression is clearly visible on the blind side of the head, but is obscured after the beginning of rapid mouth opening (by 32 ms) on the ocular side of the head.



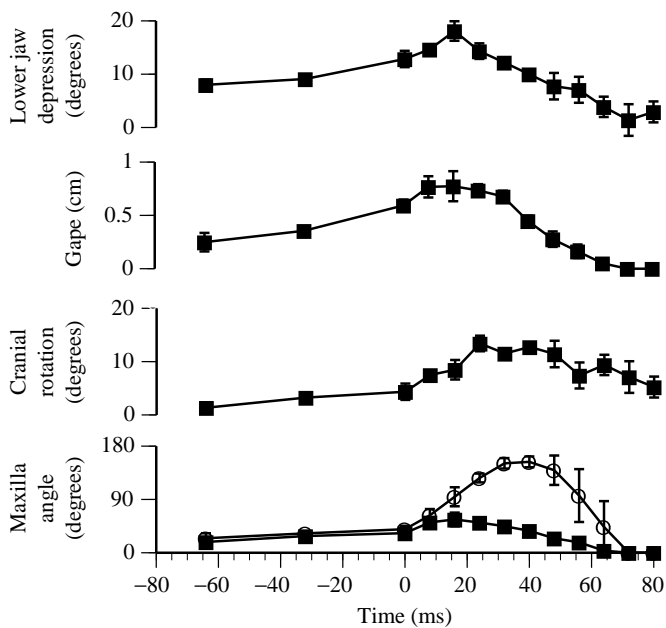


Fig. 7. Summary plot of lower jaw depression, gape, cranial rotation and maxilla angle for one sinistral *Xytreuys liolepis* (XLS2). Points on the line represent the mean values for four combined feeding sequences; error bars are one standard error of the mean. Time 0 is defined as the beginning of rapid mouth opening. Variables measured from the blind side are represented by ■; variables measured from the ocular side are represented by ○. Measurements are shown for the blind and ocular sides for maxilla angle. For clarity, only variables from the blind side are shown for gape and lower jaw depression; cranial rotation was only measured from the blind side.

development of flatfish asymmetry and handedness can answer (Policansky, 1982a,b). However, these data do suggest that reversed-symmetry individuals are not at a disadvantage in terms of the mechanics of prey capture; the jaws of reversed individuals are mirror images of their typical conspecifics, and they apparently function in the same manner.

Kinematics of prey capture

A detailed comparison of the feeding behavior of *X. liolepis* with the feeding behavior of other fishes will be given elsewhere (A. C. Gibb, in preparation). The kinematics of prey capture in *X. liolepis* will be described briefly with reference to the four phases of the feeding cycle common to actinopterygian inertial-suction feeders: the preparatory, expansive, compressive and recovery phases (Liem, 1978; Lauder, 1985). The most simple definitions of these phases are used here: the preparatory phase occurs before the mouth opens as the fish approaches the prey, the expansive phase begins when the mouth begins to open, the compressive phase begins when the mouth begins to close, and the recovery phase occurs after the mouth has closed as the head and jaws return to their original positions. In general, the prey-capture kinematics of *X. liolepis* (Figs 3, 4) demonstrate the same pattern and timing of events as seen in other actinopterygian inertial-suction feeding fishes (for a summary, see Lauder,

1985) and do not show the same modifications of this kinematic pattern previously described for *P. verticalis* (Gibb, 1995).

One unusual feature of prey capture in *X. liolepis* is the tendency of individuals to begin mouth opening during what apparently is the preparatory phase (and not the beginning of the expansive phase as traditionally defined). The mouth opens slightly and remains open for as long as 100 ms before the beginning of rapid mouth opening (Figs 3, 4). However, once rapid mouth opening begins, *X. liolepis* show a typical expansive kinematic pattern. Thus, for *X. liolepis*, the expansive phase was considered to be the period after the beginning of rapid mouth opening and was determined by the inflection point of a plot of gape versus time (e.g. see Fig. 3).

Features of *X. liolepis* prey-capture kinematics that are similar to those described for other bony fishes include the following: (1) maximum hyoid depression and maximum cranial rotation occur during the compressive phase, (2) the opercles remain expanded during the recovery phase, and (3) there is no kinematic evidence of a preparatory phase (Fig. 3). Like many other actinopterygians, individuals of *X. liolepis* do not experience a marked compressive phase of the head during the preparatory phase of the feeding cycle (Lauder, 1985). Before mouth opening begins, the opercular series is not compressed relative to its position in the same animal when it is not involved in prey-capture behavior.

The similarity of prey-capture kinematics in *X. liolepis* to that described for other actinopterygians is in contrast to previous results for another flatfish, *P. verticalis*. *P. verticalis* showed several modifications of prey-capture kinematics (including a marked preparatory phase in movements of the head and jaws) which distinguish this species from other fishes previously described (for a complete discussion of these results, see Gibb, 1995; A. C. Gibb, in preparation).

Functional asymmetry and rotation of the maxilla

Xytreuys liolepis exhibit few functional asymmetries during prey capture. They are symmetrical in most of their kinematic variables, with the exception of maximum maxilla angle. This one functional asymmetry is extreme; the angle between the rostral tips of the mandible, maxilla and premaxilla is more than twice as large on the ocular side as on the blind side (Table 5; Figs 6, 7). The functional asymmetry observed in *X. liolepis* raises an interesting question: how is this asymmetry produced?

The dorsal portion of the maxilla of most actinopterygian fishes is suspended from the neurocranium by a flexible attachment (Schaeffer and Rosen, 1961). During mouth opening, neurocranial rotation and rapid expansion of the buccal cavity, the ventral portion of the maxilla rotates anteriorly (Fig. 8). Attached to the posterior margin of the maxilla is a skin fold (pulled rostrally by the maxilla) which obscures the 'V' between the premaxilla and the mandible. This phenomenon has been described for other fishes (for example, Schaeffer and Rosen, 1961; Lauder, 1979; Aerts and Verraes, 1987) and has two hypothesized functions: (1) it could

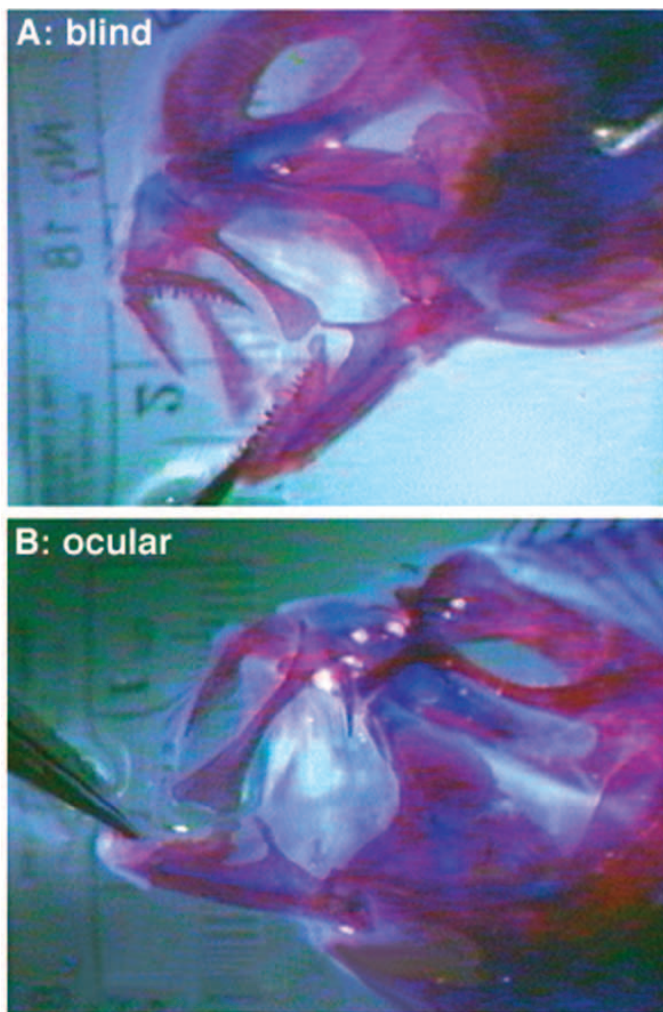


Fig. 8. Video frames showing a manipulated cleared and stained sinistral *Xystreureys liolepis*. (A) The blind side of the head; (B) the ocular side. Note that the blind side has been reversed to parallel the ocular side. The ventral portion of the maxilla appears to have moved much farther anteriorly on the ocular side than on the blind side.

prevent the escape of elusive prey items or (2) it could improve the fish's ability to direct suction at the prey. It is also possible that both functions are important.

Several possible mechanisms for the anterior rotation of the maxilla have been proposed or assumed (for example, Van Dobben, 1935; Flüchter, 1963; Alexander, 1967; Lauder, 1979; Aerts and Verraes, 1987; Westneat, 1990). In most species of fish, two obvious ligaments connect the maxilla directly to the mandible: the anterior maxilla–mandible ligament (AMML) and the posterior maxilla–mandible ligament (PMML) (see Fig. 9). The AMML connects the inner surface of the ventral portion of the maxilla to the coronoid process of the mandible. The PMML is attached to the posterior margin of the maxilla (just below the head) and to the lateral surface of the posterior portion of the mandible (the angulo-articular bone). In addition, the upper and lower jaws are attached to the maxilla by a dorsal and ventral lip ligament

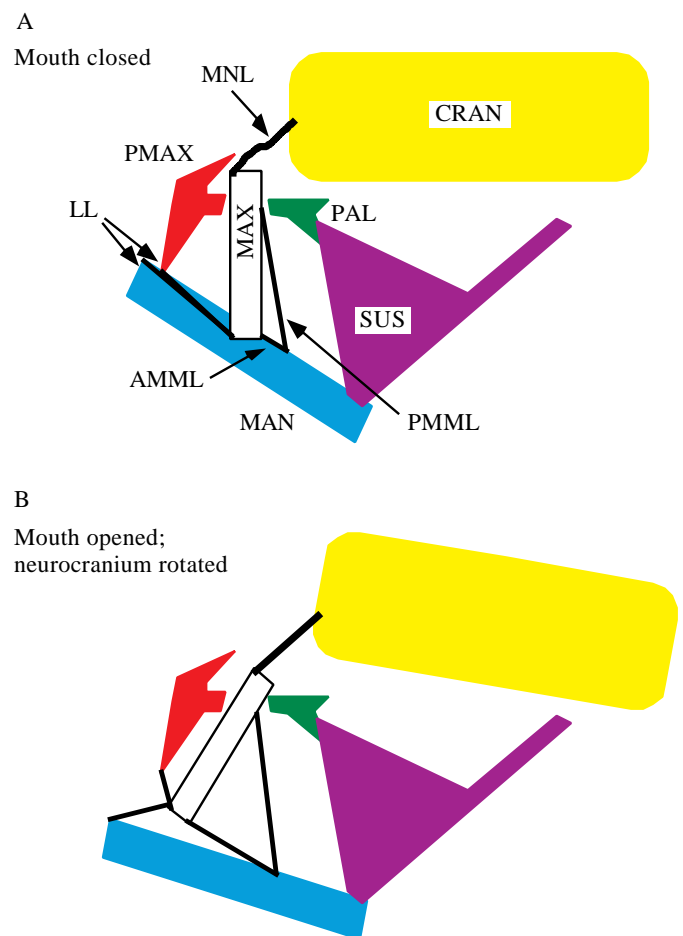


Fig. 9. Schematic model of the head of *Xystreureys liolepis* showing the relative positions of the ligaments connecting the upper and lower jaws during mouth opening. Color coding and abbreviations used in this figure are as follows: yellow, CRAN, neurocranium; red, PMAX, premaxilla; white, MAX, maxilla; blue, MAN, mandible; green, PAL, palatine; purple, SUS, suspensorium. Ligaments are indicated by black lines and are abbreviated using their initials. Lip ligaments, LL; posterior maxilla–mandible ligament, PMML; anterior maxilla–mandible ligament, AMML. Three ligaments, the maxilla–ethmoid ligament, maxilla–lacrymal ligament and lacrymal–prefrontal ligament, are shown as one (maxilla–neurocranium ligaments, MNL) and the premaxilla is shown in the same position in both panels for clarity. (A) The mouth is closed, the neurocranium is in an unrotated position, and the descending process of the maxilla is in a vertical position. (B) The mouth is open, the neurocranium has rotated dorsally, and the descending process of the maxilla has rotated anteriorly. Note that when the lower jaw is depressed the AMML and PMML will act as elastic forces resisting the anterior rotation of the ventral portion of the maxilla. Manipulation of fresh dead and preserved specimens suggests that rotation of the maxilla is produced *via* transmission of force from the neurocranium *via* the MNL. During cranial rotation, these ligaments are pulled taut as the neurocranium moves dorsally. The ligaments pull on the anterior-dorsal edge of the maxilla, causing it to rotate about its articulation with the palatine. As the head of the maxilla rotates posteriorly, the descending process rotates anteriorly.

(LL, see Fig. 9). Each of these ligaments has been implicated in the rotation of the maxilla by previous researchers.

Alexander (1967) proposed that the AMML transmits force from lower jaw depression to the maxilla. However, Lauder (1979) bilaterally transected the AMML in living individuals of both *Hoplias malabaricus* and *Oncorhynchus mykiss* (formerly *Salmo gairdneri*) and found that the maxilla swung forward to an even greater extent (indicating that the AMML actually restricts anterior movement of the maxilla). He suggested that movements ('deformation') of the neurocranium (presumably near the articulation of the maxilla) must contribute to the rostral movement of the ventral portion of the maxilla. The position of the AMML in *X. liolepis* indicates that it will impede the forward movement of the maxilla in this species as well (Fig. 9).

Van Dobben (1935) hypothesized that it was the PMML which was responsible for transmitting movement from the mandible to the maxilla during mouth opening in *Salmo salar*. However, the orientation of this ligament in many fishes, including *X. liolepis*, would seem to exclude this possibility. In *X. liolepis* when the jaws are completely closed, the ligament is slack, and initial depression of the lower jaw will cause the PMML to become taut and straighten out the maxilla. However, the ligament is attached below the point of articulation of the maxilla and the neurocranium, so once the maxilla has been rotated to this position, additional depression of the lower jaw will not continue to rotate the maxilla anteriorly. In fact, the position of the PMML in *X. liolepis* suggests that, at maximum lower jaw depression, it will act as an elastic force resisting further anterior movement of the maxilla (Fig. 9). This conclusion is supported by the fact that the tendon of adductor mandibulae 1 (a major jaw-closing muscle) inserts on this ligament, implying that the primary function of this ligament in *X. liolepis* is to close the jaws.

An additional hypothesis about the anterior movement of the maxilla was proposed by Aerts and Verraes (1987), who theorized that the initial anterior movement of the maxilla is produced by transmission of force from the lower jaw to the maxilla via the ventral lip ligament (LL). Aerts and Verraes proposed, however, that additional forward anterior movement of the maxilla (past the initial movement caused by the LL) was accomplished via inertial forces. Mathematical predictions made using kinematic and morphological parameters from *O. mykiss* appear to support their hypothesis.

Westneat (1990) proposed a similar connection between the maxilla and the lower jaw in his 'anterior jaws linkage' four-bar linkage model. This model proposed that the suspensorium acts as a fixed link, the lower jaw as an input link, the maxilla (connected by the LL to the lower jaw) as the coupler link and the palatine as the output link. In this model, depression of the lower jaw (input) creates rotation of the ventral portion of the maxilla (coupler), which pulls the palatine down (output). Subsequent movement of the anterior process of the palatine and the head of the maxilla are hypothesized to produce premaxillary protrusion. Westneat (1990) constructed predictive models using morphological measurements and the four-bar linkage to predict jaw movements. Kinematic measurements obtained during feeding in two species of

Cheilinus supported his hypotheses about the mechanical structure of the anterior jaws; the anterior jaws linkage model was apparently an accurate predictor of jaw movements.

Transecting any or all of these ligaments (the PMML, the AMML and both portions of the LL) in fresh dead specimens does not impede forward movement of the ventral portion of the maxilla. Since transecting these ligaments eliminates any direct connection between the upper and lower jaw, this implies that the lower jaw is not responsible for maxilla rotation in *X. liolepis*. When all of the ligaments and skin connecting the ventral portion of the maxilla and the lower jaw are removed, the ventral portion of the maxilla still rotates anteriorly when the neurocranium is manually rotated dorsally. Thus, for *X. liolepis*, it appears that it is the neurocranium, and not the lower jaw, which transmits force to the maxilla and the premaxilla.

Multiple ligaments connect the rostral region of the neurocranium to the head of the maxilla in flatfishes (Flüchter, 1963). However, three ligaments are located in a position to rotate the maxilla via movement of the neurocranium: the maxilla-ethmoid ligament, the maxilla-lacrymal ligament and the lacrymal-prefrontal ligament. The maxilla-ethmoid ligament is attached to the anterior rim of the head of the maxilla and extends dorsally and attaches to the ethmoid region of the skull. The maxilla-lacrymal ligament is also connected to the anterior rim of the head of the maxilla. It attaches to the lacrymal bone, where it connects with the lacrymal-prefrontal ligament, which in turn attaches to the prefrontal region of the skull. These ligaments will be referred to collectively as the maxilla-neurocranium ligaments (MNL).

In an unmanipulated fresh dead specimen, these three ligaments connecting the head of the maxilla to the skull are slack when the mouth is closed (these ligaments are shown schematically as one ligament in Fig. 9A). However, when the neurocranium is manually rotated dorsally in a fresh dead specimen, these ligaments become taut and pull the head of the maxilla posteriorly and dorsally. Consequently, the maxilla rotates about its articulation with the palatine bone and the rotation about this articulation causes the descending portion of the maxilla to move anteriorly (Fig. 9B). This model is supported by two pieces of empirical evidence: (1) when the MNLs are cut in fresh dead animals and the neurocranium is manually rotated dorsally, anterior movement of the ventral portion of the maxilla is significantly reduced, and (2) maximum maxilla rotation (as measured by maxilla angle) occurs at the same time as maximum rotation of the neurocranium (Fig. 7).

Relatively little work has been carried out on the jaw mechanisms of flatfish, but much of that work has been focused on *Pleuronectes platessa* (Van Dobben, 1935; Flüchter, 1963; Alexander, 1967; Yazdani, 1969). Flüchter (1963) and Alexander (1967) both noted that it is very difficult to reduce premaxillary protrusion (and maxillary rotation) in dead specimens by cutting the ligaments connecting the upper and lower jaw of this species. In addition, Flüchter (1963) proposed that the palatine plays a particularly important role in blocking

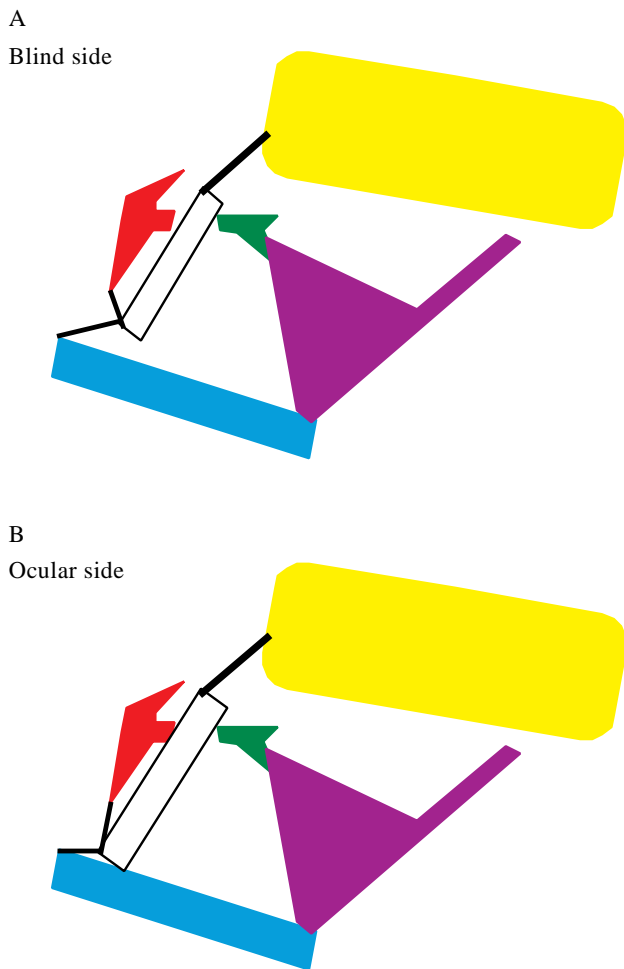


Fig. 10. Simple model of the jaw apparatus of *Xystreureys liolepis* including asymmetry in the length of the maxilla for (A) the blind side of the head and (B) the ocular side. The blind side has been reversed horizontally in order to facilitate comparisons with the ocular side. Bones and ligaments are color-coded as in Fig. 9. The maxilla on the blind side is approximately 90% of the length of the maxilla on the ocular side (see Fig. 2); all other schematic components are the same length in both panels. This simple model demonstrates that dorsal rotation of the neurocranium will produce a different maxilla angle (the angle between the rostral tips of the mandible, maxilla and premaxilla) on the two sides of the head ($>90^\circ$ on the ocular side, $<90^\circ$ on the blind side) simply because of the asymmetry in maxilla length.

posterior movement of the maxilla on the ocular side of *P. platessa*. Thus, previous research on flatfish jaws supports the idea that this mechanism of maxilla rotation could be common among flatfish species.

It is not clear how widespread this mechanism of maxillary rotation is among other less specialized fish taxa. However, it is interesting to note that this hypothesis closely parallels Lauder's (1979) suggestion that maxillary rotation is caused by movements of the neurocranium in *H. malabaricus* and *O. mykiss*.

No matter which mechanism actually generates rotation of

the maxilla, it appears that the difference in length between the ocular- and blind-side maxillae (Figs 2, 8) is sufficient to explain the observed difference in maximum maxilla angle. Fig. 10 illustrates that the blind-side maxilla (which is only 90% the length of the ocular-side maxilla) will not move as far anteriorly as the longer maxilla on the ocular side, simply because it is shorter. This very simple model suggests that the asymmetrical length of the maxilla is all that is required to produce the asymmetrical maximum maxilla angle measured in *X. liolepis*.

Asymmetry of the palatine bone in this species (Fig. 2) supports the hypothesis that the palatine plays an important role in the rotation of the maxilla. The neurocranium-mediated model of maxilla rotation emphasizes the importance of the palatine bone as a fulcrum for the maxilla. In addition, lateral expansion of the suspensorium during prey capture probably changes the articulation of the anterior process of the palatine with the head of the maxilla. Thus, the difference in the shape of the anterior process of the palatine and the head of the maxilla on the ocular and blind sides (Fig. 2) may create a different movement in the maxilla on the two sides of the head. A more detailed analysis of the morphological asymmetry of this species will be necessary to determine the extent to which this plays a role in the functional asymmetry observed in *X. liolepis*.

However, this preliminary model created using morphological characteristics suggests that morphological asymmetry is sufficient to explain functional asymmetry in *X. liolepis*. Thus, this model implies that asymmetry of the neuromuscular control of bones of the head and jaws is not necessary to produce the observed functional asymmetry. Research currently under way will directly address the potential contribution of neuromuscular asymmetry to functional asymmetry by examining muscle activity patterns during feeding in flatfish.

Do all flatfish feed asymmetrically?

The prey-capture kinematics of *X. liolepis* do exhibit functional asymmetry, but they exhibit a very different pattern of functional asymmetry from that found in the previously studied species of flatfish, *Pleuronichthys verticalis*. *P. verticalis* exhibit asymmetry in maximum gape and extreme lateral flexion of the jaws towards the blind side. These modifications apparently allow this species of flatfish to direct the suction generated during prey capture at their potential prey. *Xystreureys liolepis*, in contrast, produce an asymmetrical maximum maxilla angle during prey capture. The asymmetrical movement of the maxilla eliminates the 'V' created by mouth opening on the ocular side and probably blocks one potential escape route of the prey item.

Both flatfish species examined thus far exhibit some functional asymmetry during prey capture, but the type of asymmetry is quite different in the two taxa studied. The results of this study indicate that there is no stereotypical pattern of flatfish functional asymmetry; it appears that functional asymmetry varies across taxa along with morphological

asymmetry. These results also suggest that certain morphological asymmetries of the jaws of flatfishes are modifications for specialized prey-capture behaviors.

This research was supported by a University of California Natural Reserve Research Grant and California Sea Grant College Graduate Research Fellowship to A.C.G., as well as NSF grant IBN 91-19502 to George Lauder. Jim Allen of SCWRP provided essential information on the morphology and ecology of local flatfish species and Miriam Ashley-Ross provided invaluable technical assistance during the video-taping. I also thank Miriam Ashley-Ross, Heidi Doan, Lara Ferry, Allen Gibbs, Gary Gillis, George Lauder, Larry MacPhee and the two anonymous reviewers for helpful comments on the manuscript.

References

- AERTS, P. AND VERRAES, W. (1987). Do inertial effects explain the maximal rotation of the maxilla in the rainbow trout (*Salmo gairdneri*) during feeding? *Annls Soc. R. Zool. Belg.* **117**, 221–235.
- AHLSTROM, E. H., AMAOKA, K., HENSLEY, D. A., MOSER, H. G. AND SUMIDA, B. Y. (1984). Pleuronectiformes: development. In *Ontogeny and Systematics of Fishes*, Special Publication 1, American Society of Ichthyologists and Herpetologists (ed. H. G. Moser), pp. 640–670. Lawrence, KS: Allen Press.
- ALEXANDER, R. M. (1967). The functions and mechanisms of the protrusible upper jaws of some acanthopterygian fish. *J. Zool., Lond.* **151**, 43–64.
- ALLEN, M. J. (1982). Functional structure of soft-bottom fish communities of the southern California shelf, pp. 577. PhD dissertation. La Jolla, CA, University of California, San Diego.
- CHAPLEAU, F. (1993). Pleuronectiform relationships: a cladistic reassessment. *Bull. mar. Sci.* **51**, 516–539.
- FLÜCHTER, J. (1963). Funktionell-morphologische Untersuchungen über die Kieferapparate einiger Plattfische. *Zool. Beitr.* **8**, 23–94.
- GIBB, A. C. (1995). Kinematics of prey capture in a flatfish, *Pleuronichthys verticalis*. *J. exp. Biol.* **198**, 1173–1183.
- GINSBURG, I. (1952). Flounders of the genus *Paralichthys* and related genera in American waters. *Fishery Bull. Fish Wildl. Serv. U.S.* **52**, 265–351.
- HUBBS, C. L. AND HUBBS, L. C. (1945). Bilateral asymmetry and bilateral variation in fishes. *Pap. Mich. Acad. Sci., Arts Lett.* **30**, 229–310.
- KRAMER, S. H. (1991). The shallow-water flatfishes of San Diego county. *Cal. COFI Rep.* **32**, 128–142.
- LAUDER, G. V. (1979). Feeding mechanics in primitive teleosts and in the halecomorph fish *Amia calva*. *J. Zool., Lond.* **187**, 543–578.
- LAUDER, G. V. (1985). Aquatic feeding in lower vertebrates. In *Functional Vertebrate Morphology* (ed. M. Hildebrand, D. M. Bramble, K. F. Liem and D. B. Wake), pp. 210–229. Cambridge: Harvard University Press.
- LIEM, K. F. (1978). Modulatory multiplicity in the functional repertoire of the feeding mechanism in cichlid fishes. I. Piscivores. *J. Morph.* **158**, 323–359.
- POLICANSKY, D. (1982a). The asymmetry of flounders. *Scient. Am.* **246**, 116–122.
- POLICANSKY, D. (1982b). Flatfish and the inheritance of asymmetries. *Behav. Brain Sci.* **5**, 262–265.
- RICE, W. R. (1989). Analyzing tables of statistical tests. *Evolution* **43**, 223–225.
- RICHARD, B. A. AND WAINWRIGHT, P. C. (1995). Scaling the feeding mechanism of largemouth bass (*Micropterus salmoides*): kinematics of prey capture. *J. exp. Biol.* **198**, 419–433.
- SCHAEFFER, B. AND ROSEN, D. E. (1961). Major adaptive levels in the evolution of the actinopterygian feeding mechanism. *Am. Zool.* **1**, 187–204.
- VAN DOBBEN, W. H. (1935). Über den Kiefermechanismus der Knochenfische. *Arch. neerl. Zool.* **2**, 1–72.
- WESTNEAT, M. W. (1990). Feeding mechanics of teleost fishes (Labridae; Perciformes): a test of four-bar linkage models. *J. Morph.* **205**, 269–295.
- YAZDANI, G. M. (1969). Adaptations in the jaws of flatfish (Pleuronectiformes). *J. Zool., Lond.* **159**, 181–222.